Microchemical Journal 95 (2010) 293–297

Contents lists available at ScienceDirect

Microchemical Journal

journal homepage: www.elsevier.com/locate/microc

The performance of a fast testing system for illicit materials detection based on energy-dispersive X-ray diffraction technique

Bai Sun, Minqiang Li, Fang Zhang, Yu Zhong, Nansheng Kang, Wei Lu, Jinhuai Liu *

The Key Laboratory of Biomimetic Sensing and Advanced Robot Technology, Anhui Province, Institute of Intelligent Machines, Chinese Academy of Sciences, Hefei, 230031, PR China

ARTICLE INFO

Article history:
Received 11 November 2009
Received in revised form 29 December 2009
Accepted 29 December 2009
Available online 7 January 2010

Keywords:
X-ray
Energy dispersive
Nondestructive detecting
Explosives
Drugs
EDXRD

ABSTRACT

A prototype setup for detecting illicit materials by energy-dispersive X-ray diffraction (EDXRD) has been developed. The obtained results of NaCl by the equipment suggest that the total measurement system is reliable and can be used to detect different kinds of materials. The tests of TNT, methamphetamine and heroin are also performed on this equipment and the related EDXRD spectra are obviously influenced by the detecting angle and the X-ray sources. The detecting angle of 10° is more suitable for detecting TNT and methamphetamine, while 12° is better for heroin. Moreover, the curves of TNT, methamphetamine and heroin emitted by W target have more diffraction peaks than those emitted by Cu or Mo target, while the peak intensities of TNT and methamphetamine emitted by Mo are stronger than those emitted by Cu or W target. The curve of methamphetamine emitted by Mo target shows a special characteristic and exhibits a super strong diffraction peak located at 1.62 $Å^{-1}$, which can be attributed to the effect arising from Mo kα and kβ.

1. Introduction

Recently, applications to the inspection related to security and safety are strongly required because of serious social and political situations in the world. After the 9-11-2001 attack on New York's World Trade Center, the American Federal Government and the European Civil Aviation Conference (ECAC) have demanded 100% inspection of hold luggages at all airports for security consideration, which induces insupportable low clearance efficiency. In addition, the illegal drugs hidden in sealed envelopes for both domestical delivery and international smuggle become more and more serious security issues for many countries. However, there is still no effective method to detect those hidden drugs in sealed envelopes nondestructively, as the opening of sealed envelope without a search warrant is always prohibited by law. Obviously, for security reasons, practical detection technologies are aspired for the nondestructive and fast detection for those dangerous and illegal items.

Currently, different detection techniques for illicit materials have been developed, such as acoustic detector technology [1], neutron/gamma-ray scattering analysis [2–4], and different X-ray inspection techniques including X-ray dual-energy transmission and scatter technologies [5,6] and energy-dispersive X-ray diffraction method (EDXRD) [7–10]. Among them, EDXRD method has been considered to be the suitable nondestructive method to rapidly identify different illegal materials, which can satisfy the above security requests. This technology is based on the measurement of energy-dispersive low angle scattering of photons from a polychromatic incident beam. For EDXRD testing, the EDXRD spectrum is a diffraction profile from the scattering media, which is unique to that particular material and can be regarded as the "fingerprint" of the testing object. Because of its unique characterization and advantages, this nondestructive technique has demonstrated to be promising for the detection and identification of explosives and drugs within luggage effectively [11–14]. Furthermore, for EDXRD technology, a goniometer for the exact measurement of different diffraction angles is not necessary and the measurement time can be greatly reduced with respect to the traditional angular dispersive techniques [15]. So equipped with a small power X-ray tube as the appropriate X-ray source and a high energy resolution detector for the diffracted beam, a small and transportable testing equipment can be constructed, which supplies a mobile and convenient measurement for process analysis applications [16].

In this study, a prototype analyzer for detecting illicit materials based on EDXRD has been developed and the reliable performance of investigating NaCl, TNT, methamphetamine (ice) and heroin has been demonstrated.

2. Theories and experimental details

The atoms in crystalline materials are arranged in such a way that regularly spaced atomic planes can be identified. The Bragg's law gives the relationship between the X-ray wavelength λ, the scatter angle θ

* Corresponding author. Fax: +86 551 5592420.
E-mail address: jhliu@iim.ac.cn (J. Liu).

0026-265X/$ – see front matter © 2010 Elsevier B.V. All rights reserved.
doi:10.1016/j.microc.2009.12.018

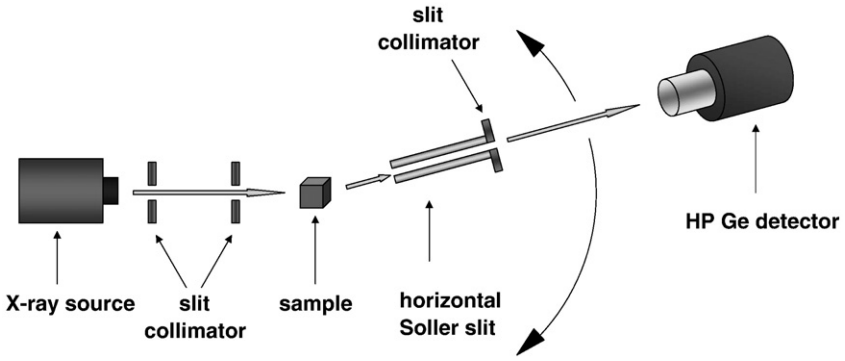

Fig. 1. Schematic representation of an EDXRD spectrometer.

and an atomic planar spacing (lattice spacing) d of the investigated material, which has to be fulfilled for positive interference:

$$2d\sin\frac{\theta}{2} = n\lambda. \quad (1)$$

In the case of EDXRD, it is more convenient to write Eq. (1) in terms of the X-ray energy rather than the wavelength:

$$2d\sin\frac{\theta}{2} = \frac{nhc}{E} \quad (2)$$

here h is Planck's constant, c is velocity of light, λ is replaced by the photon energy E. Obviously a primary X-ray photon with high energy is scattered under a small scatter angle θ for a given lattice spacing d. Since the scatter angle is fixed, different lattice spacings characterizing the crystalline structure of the material result in different diffraction peaks within the energy spectrum of the scattered X-ray photons. According to the Bragg-condition the spectrum will be shifted along the energy axis if the scatter angle is changed. It will be shown below that the spectral resolution and the ability to distinguish different diffraction peaks are strongly influenced by the choice of the scatter angle. By means of the Bragg-condition (2) the peak positions E within the normalized spectrum can be used to calculate the corresponding lattice spacing d by comparison with literature data (Powder Diffraction File). On the other hand the peak positions of a material within the energy spectrum measured in this experiment can be predicted from the peaks of the angular dispersive PDF-data using the same equations.

In order to compare results from different systems, the diffraction profile is expressed as a function of momentum transfer q, which depends on both the photon energy (E) and scatter angle as follows:

$$q = CE\sin\left(\frac{\theta}{2}\right). \quad (3)$$

$C = 1.01354\ \text{Å}^{-1}\,\text{keV}^{-1}$. The ability of the system to resolve the peaks in momentum transfer space depends on the angular resolution of the diffraction cell and the energy resolution of the detector.

An EDXRD spectrometer consists of a polychromatic source of X-ray and an energy-resolving detector as shown in Fig. 1. The polychromatic source of X-ray typically comprises an X-ray tube and the related collimators to define the incident and scattered beams. Cu, W or Mo target is chosen as the X-ray source in the range 0–60 kV and 0–30 mA. The focal spot is 3 mm with a 3 mm entrance aperture. The primary and scattered beams are both collimated with slits collimation, which provides an increased flux over pencil beam collimation, while maintaining acceptable angular resolution in the horizontal plane. For the EDXRD apparatus, a solid-state liquid-nitrogen-cooled high purity germanium (HP Ge) detector with sufficient energy resolution is adopted. The Canberra planar HP Ge detector with 50 mm^2 detector area and 5 mm thick has a resolution of 120 eV at 5.9 keV combined with a Canberra spectrum master InSpector 2000. The incident and scattered beam collimation is formed by interlocking leaf collimators 50 mm in height and of variable slit width. The incident beam collimation forms a ribbon beam, 16 mm in height, at the sample. The detector collimation can be orientated at any selected angle relative to the incident beam and the slit width varied according to the required angular resolution. The peculiar design of the instrumental components allows placing big samples in the centre of the instrument in such a way that the area to be investigated is in the optical focus. It has to be underlined that the exact positioning of the area of the sample in the focus is a necessary step to avoid distortion on the diffraction peaks. During the measurements, the X-ray tube and the specimen are maintained fixed, whereas the detector can rotate around the centre of the goniometer where the sample is placed. Another peculiarity of the instrument is the possibility of making measurements either in transmission or in reflection geometry. This important feature allows obtaining information about the surface layers of a sample.

3. Result and discussion

3.1. Accuracy of the measurements

In order to demonstrate the potential of the apparatus based on the energy-dispersive X-ray diffraction method, W target was chosen as the X-ray source and NaCl as the sample. During the experiment, the testing samples, without collection of any portion and without any preliminary preparation, were placed in the instrument. Spectra were collected in a wide energy range that contains X-ray diffraction features. The diffracted X-ray is collected in transmission mode and the measurement time for each spectrum is 5 min. The operational voltage and current of the X-ray tube are 40 kV and 30 mA, respectively. The above operational conditions keep constant for all

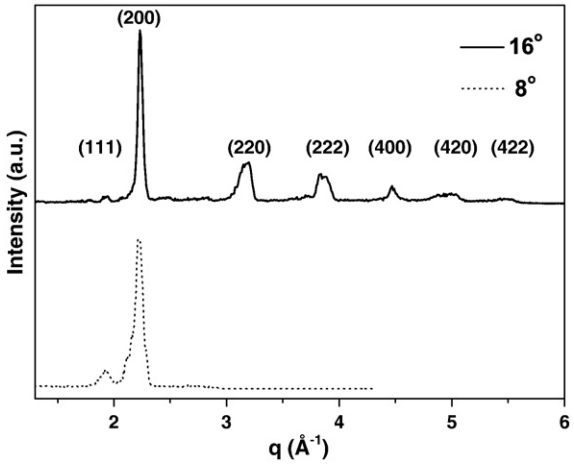

Fig. 2. The diffraction patterns of NaCl, detecting angles are 8° and 16°.

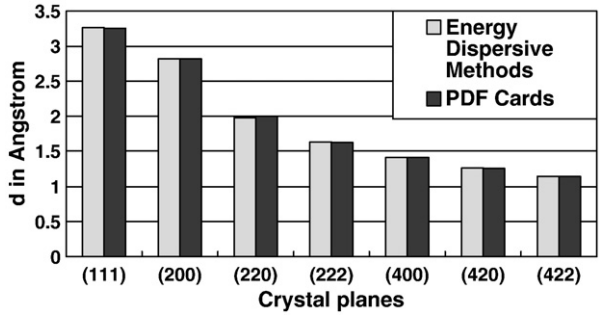

Fig. 3. Comparison of the experimental results and the standard X-ray diffraction data — PDF (Powder Diffraction File) issued by the International Centre for Diffraction Data.

of the testing samples here. The diffraction patterns of the NaCl are given in Fig. 2. The testing range of the profile detected at 8° and 16° are 1.3 to 4.3 $Å^{-1}$ and 1.3 to 6.0 $Å^{-1}$ respectively. For the spectrum detected at 8°, there are only two diffraction peaks in the curve with the positions of 1.94 $Å^{-1}$ and 2.22 $Å^{-1}$, which correspond to NaCl (111) and (200) crystal plane respectively. For the spectrum detected at 16°, there are seven diffraction peaks in the curve. Besides the mentioned peaks located at 1.94 $Å^{-1}$ and 2.22 $Å^{-1}$, another five diffraction peaks located at 3.17 $Å^{-1}$, 3.86 $Å^{-1}$, 4.47 $Å^{-1}$, 4.98 $Å^{-1}$, and 5.47 $Å^{-1}$ correspond to the (220), (222), (400), (420), and (422) crystal plane of NaCl, respectively. The corresponding *d* values for these diffraction peaks can be calculated using the Bragg's law. Fig. 3 shows the comparison between the experimental results and the standard X-ray diffraction data — PDF (Powder Diffraction File) issued by the International Centre for Diffraction Data. It can be observed that the *d* values obtained from the experiments are consistent with the values on the PDF card, confirming the reliability of the results obtained by our apparatus. The total measurement system can thus be used to detect different kinds of materials based on energy-dispersive X-ray diffraction method.

3.2. Influence of detecting angle on the diffraction profiles of the illicit materials

Fig. 4 shows the EDXRD patterns of the TNT measured at detecting angles of 8°, 10°, 12°, 14° and 16° emitted by W target. There are three diffraction peaks in each EDXRD curve of TNT, and the most intense peak is located at 1.64 $Å^{-1}$. It can be seen that with the detecting angle increasing, the intensities of the diffraction peaks increase to a

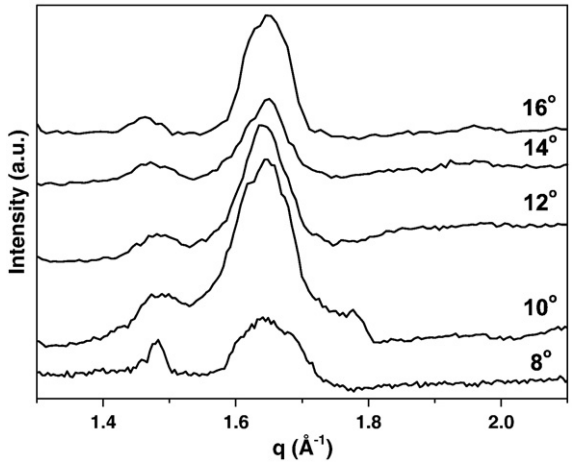

Fig. 4. The diffraction patterns of TNT, detecting angles are 8°, 10°, 12°, 14° and 16°.

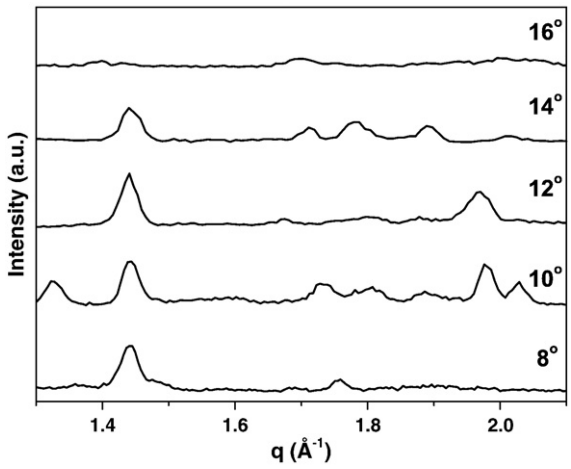

Fig. 5. The diffraction patterns of methamphetamine, detecting angles are 8°, 10°, 12°, 14° and 16°.

maximal value at 10°, followed by a decrease. The FWHM value of the diffraction peak located at 1.64 $Å^{-1}$ in the curve detected at 10° is the smallest, suggesting the detecting angle of 10° is more suitable to detect TNT. So the further work of TNT was carried out at the detecting angle of 10°.

The EDXRD curves of the methamphetamine detected at different angles (8°, 10°, 12°, 14° and 16°) are shown in Fig. 5, where W target is used as the X-ray source. In the curves detected at the angles of 8°, 10° and 12°, the strongest peaks located at 1.44 $Å^{-1}$ and the intensities of them are almost the same. However, for the detecting angle of 14°, the intensity of the strongest peak is weaker than those in the other curves. When the detecting angle increased to 16°, the intensities of all the diffraction peaks decreased dramatically. In addition, the diffraction curve detected at 10° has the most number of the diffraction peaks; therefore, the scatter angle of 10° was chosen for the further work of methamphetamine.

Using W target as the X-ray source, the EDXRD spectra of heroin tested with the detecting angles from 8 to 16° are plotted in Fig. 6. In these spectra the ratios of the signal to the noise are lower than that of TNT and methamphetamine due to the poor crystallizability of the heroin. Considering the intensity, the momentum transfer resolution and the number of the diffraction peaks, the spectrum with the scatter angle of 12° shows two most prominent peaks at 1.65 and 1.85 $Å^{-1}$,

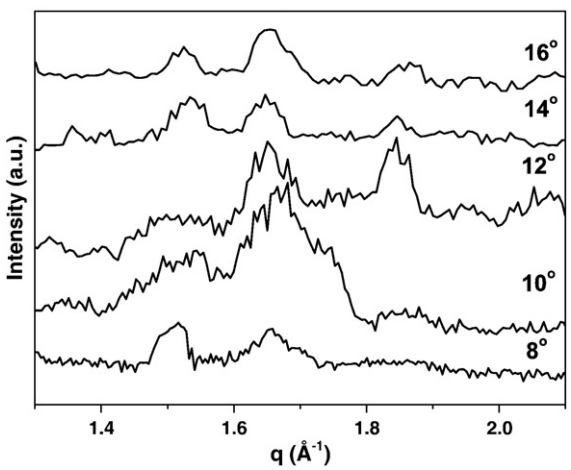

Fig. 6. The diffraction patterns of heroin, detecting angles are 8°, 10°, 12°, 14° and 16°.

and the scatter angle of 12° was thus chosen as the suitable parameter for the further work of heroin.

From the above statement, the EDXRD curves of the TNT and methamphetamine detected at 10° have the stronger diffraction peaks and much more diffraction peaks, while for the heroin, the curve detected at 12° has the stronger diffraction peaks and much more diffraction peaks. It is understandable as X-ray beam mean penetration depth is seriously depending on the X-ray energy, the radiation incidence angle and the elemental composition of the testing samples. Therefore, the profiles and intensities of the EDXRD curves of the TNT, methamphetamine and heroin are quite different with different detecting angles.

3.3. The effect of X-ray sources

The bremsstrahlung distribution of photons emitted by an X-ray tube depends on the following terms: material of the anode, anode geometry (electron incidence angle and photon take-off angle), operating voltage of the X-ray tube, contamination of the anode, and impurities of the anode material. In order to investigate the influence of different X-ray sources on detecting the illicit materials by the EDXRD, W, Cu and Mo targets based X-ray sources are applied for the following testing. The detecting angle of 10° was selected for TNT and methamphetamine, and the detecting angle of 12° for heroin. The EDXRD patterns of the TNT emitted by W, Cu and Mo targets detected at 10° are shown in Fig. 7. Four diffraction peaks in the curve emitted by Cu target are observed for the values of 1.13 $Å^{-1}$, 1.28 $Å^{-1}$, 1.49 $Å^{-1}$ and 1.64 $Å^{-1}$, the corresponding interatomic distances can be estimated to be 5.56 Å, 4.94 Å,4.22 Å and 3.83 Å, which are associated with the d_{230},d_{221} and d_{150} spacing distances of the TNT, whereas, the value 5.56 Å could be attributed to the different preparing techniques or the impurity of the TNT sample. Furthermore, there exists extra obvious diffraction peak located at 1.78 $Å^{-1}$ in the curve emitted by W target except those four diffraction peaks appeared in the curve emitted by Cu target, which coincided with the (340) crystal plane of TNT. The intensities of the diffraction peaks in the curve emitted by W target are also stronger than those emitted by Cu target. In addition, two special stronger peaks located at 1.54 $Å^{-1}$ and 1.73 $Å^{-1}$ appear in the curve emitted by Mo target, the two stronger peaks are attributed to the Mo kα and kβ. The intensities of the diffraction peaks in the curve emitted by Mo target are stronger than those in the curves emitted by Cu target and W target, especially the peak located at 1.64 $Å^{-1}$ between the Mo kα and kβ in the curve emitted by Mo target is much stronger than those in the curves emitted by Cu target and W target.

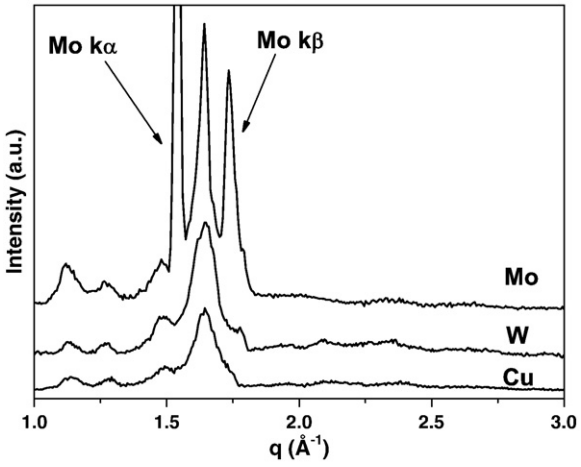

Fig. 7. The EDXRD patterns of the TNT emitted by W, Cu and Mo targets detected at 10°.

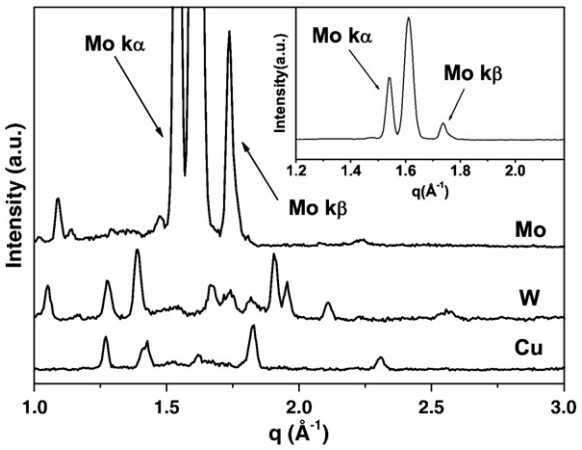

Fig. 8. The EDXRD patterns of the methamphetamine emitted by W, Cu and Mo targets detected at 10°.

The EDXRD patterns of the methamphetamine emitted by W, Cu and Mo targets detected at 10° are shown in Fig. 8. In the curve emitted by Cu target, there are five diffraction peaks located at 1.26 $Å^{-1}$, 1.41 $Å^{-1}$, 1.62 $Å^{-1}$, 1.82 $Å^{-1}$ and 2.31 $Å^{-1}$, according to the methamphetamine crystal plane (011), (111), ($\bar{2}$11), (120) and (221), whereas in the curve emitted by W, the number of the diffraction peaks is more than that in the curve emitted by Cu. Moreover, the intensities of the diffraction peaks are stronger than those in the curve emitted by Cu. In the curve emitted by Mo target, the number of the diffraction peaks is fewer than that in the curves emitted by Cu target and W target. However, an absorbing phenomenon appeared in the curve emitted by Mo target, there is a very strong diffraction peak located at 1.62 $Å^{-1}$ between the Mo kα and kβ, which corresponds to the ($\bar{2}$11) crystal plane of methamphetamine. It is even stronger than Mo kα and kβ, as shown in the inset of Fig. 8. This phenomenon hasn't been reported in the previous literatures. It could be understandable as the position of the super strong diffraction peak near the Mo kα and kβ, the diffraction peaks were emitted not only by the bremsstrahlung of the Mo target, but also emitted by the Mo kα and kβ.

Why do the curves of methamphetamine emitted by different X-ray sources have different profiles besides the X-ray tube anode element fluorescence peaks (Mo kα and kβ)? The number of diffraction peaks of methamphetamine emitted by Cu target, W target and Mo target is W>Cu>Mo, which could be attributed to the fact that bremsstrahlung of W target is stronger than that of the Cu and Mo targets between the q range from 1.0 $Å^{-1}$ to 3.0 $Å^{-1}$ at detecting angle 10° [17]. On the other hand, the crystallizability of methamphetamine is very good, so the tested methamphetamine sample here is more easier to be in the form of crystal, which can make it possible to appear super strong diffraction peaks.

The EDXRD patterns of the heroin detected at 12° emitted by Cu, W and Mo targets are plotted in Fig. 9. All EDXRD scans contain the relevant peaks of the crystalline forms of heroin, within the investigated q-range, there are five diffraction peaks of heroin in the curve emitted by Cu target, their positions are 1.19 $Å^{-1}$, 1.53 $Å^{-1}$, 1.66 $Å^{-1}$, 1.84 $Å^{-1}$ and 2.10 $Å^{-1}$, which correspond to the (112), (032), (123), (221) and (105) crystal plane of heroin respectively. As the X-ray source changes from Cu target to W target, the profiles and the positions of the diffraction peaks are similar, nevertheless the intensities of the diffraction peaks change. The diffraction peaks emitted by W target are stronger than those emitted by Cu target. In the measured curves using the Mo target as the X-ray source, the peaks located at 1.19 $Å^{-1}$ deteriorated, whereas the peaks located at 1.84 $Å^{-1}$ and 2.10 $Å^{-1}$ increased obviously, which is attributed to the fact that the element of the X-ray target fluorescence peaks cover up

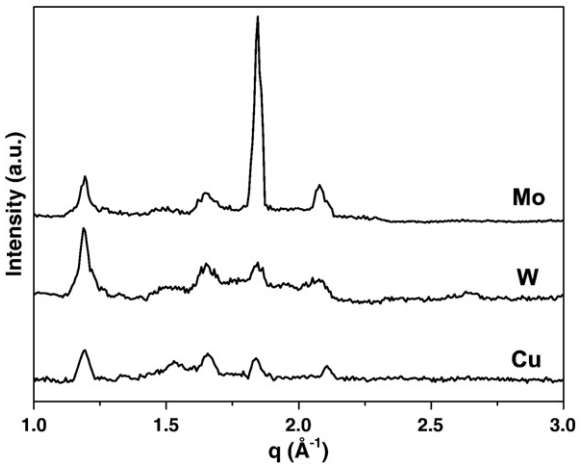

Fig. 9. The EDXRD patterns of the heroin emitted by Cu, W and Mo targets detected at 12°.

the valuable signal. For the detection of heroin, the intensities of the diffraction peaks obtained using the W target as the X-ray source are stronger than those in the curves obtained using the Cu or Mo target as the X-ray source. On the other hand, at the detecting angle 12°, the Mo kα and kβ fluorescence peaks envelop the diffraction peaks which are used as the evidence to inspect heroin; therefore, the W target is more suitable for detecting heroin at 12° compared with the Cu and Mo targets.

For the EDXRD patterns of the TNT and methamphetamine emitted by Cu, W and Mo targets at the detecting angle of 10°, the Mo kα and kβ affect the profiles of the curves remarkably. The presence of the Mo kα and kβ in the range of q value 1.0 $Å^{-1}$ to 3.0 $Å^{-1}$ will interfere with the measured diffraction peaks. However, they can obviously enhance the intensities of the diffraction peaks and then improve the sensitivity to detect the illicit materials. In addition, for practical application, choosing suitable detecting angle could avoid the overlap between the diffraction peaks from the testing samples and the fluorescence peaks of the X-ray target effectively. Furthermore, it could enhance the intensity of the testing signal, increasing the detection limit and sensitivity to illicit materials by EDXRD method.

4. Conclusion

A prototype analyzer for detecting illicit materials (TNT, methamphetamine and heroin) based on EDXRD method has been developed. The results of NaCl obtained by the equipment suggest that the total measurement system can be used to detect different kinds of materials. The EDXRD curves of TNT, methamphetamine and heroin are obviously influenced by the detecting angles and the X-ray sources. The detecting angle of 10° is more suitable for detecting TNT and methamphetamine, while 12° is better for heroin. The choice of X-ray source with suitable target is another important factor for the performance of illicit materials testing based on EDXRD method. According to our results, the curves of TNT, methamphetamine and heroin emitted by W target have more diffraction peaks than those emitted by Cu and Mo targets, which suggests the evidences used to distinguish illicit materials are more sufficient to enhance the detecting accuracy. In the curve emitted by Mo target, the Mo kα and kβ affect the profile curves remarkably. The presence of the Mo kα and kβ in the range of q value 1.0 $Å^{-1}$ to 3.0 $Å^{-1}$ will partially overlap the diffraction signals. However, they can obviously enhance the intensities of the diffraction peaks, improving the sensitivity to detect the illicit materials. Obviously, for practical application of EDXRD method, choosing suitable detecting angle could enhance the intensity of the signal for increasing the detection limit and sensitivity as well as avoiding the overlap of the fluorescence peaks from the X-ray source.

Acknowledgement

This work was financially supported by the Key Program of National Natural Science Foundation of China (Grant 10635070).

References

[1] R.D. George, R.D. Gauthier, K.D. Denslow, A.M. Cinson, A.A. Diaz, M. Griffin, Contraband detection using acoustic technology, Proc. SPIE 6934 (2008) 693415.
[2] H.S. Lee, S.R. Park, B.Y. Lee, S.K. KO, C.W. Chung, Study on detection technique of illicit materials using pulsed fast white neutron analysis, Nucl. Instrum. Methods A 562 (2006) 1076–1080.
[3] A. Buffler, F.D. Brooks, M.S. Allie, K. Bharuth-Ram, M.R. Nchodu, Material classification by fast neutron scattering, Nucl. Instrum. Methods B 173 (2001) 483–502.
[4] H.J. Im, K. Song, Applications of prompt gamma ray neutron activation analysis: detection of illicit materials, Appl. Spectrosc. Rev. 44 (4) (2009) 317–334.
[5] Q. Lu, The Utility of X-ray Dual-energy Transmission and Scatter Technologies for Illicit Material Detection, Virginia Polytechnic Institute and State University, Blacksburg, Virginia, August, Doctor's Thesis, 1999.
[6] S. Singh, M. Singh, Explosives detection systems (EDS) for aviation security, Signal Process. 83 (2003) 31–55.
[7] E. Cook, R. Fong, J. Horrocks, D. Wilkinson, R. Speller, Energy dispersive X-ray diffraction as a means to identify illicit materials: a preliminary optimisation study, Appl. Radiat. Isot. 65 (8) (2007) 959–967.
[8] B. Kämpfe, F. Luczak, B. Michel, Energy dispersive X-ray diffraction, Part. Part. Syst. Charact. 22 (6) (2005) 391–396.
[9] E.J. Cook, J.A. Griffiths, M. Koutalonis, C. Gent, S. Pani, J.A. Horrocks, L. George, S. Hardwick, R. Speller, Illicit drug detection using energy dispersive X-ray diffraction, non-intrusive inspection technologies II, Proc. SPIE 7310 (2009) 73100I.
[10] E.J. Cook, S. Pani, L. George, S. Hardwick, J.A. Horrocks, R.D. Speller, Multivariate data analysis for drug identification using energy-dispersive X-ray diffraction, IEEE T, Nucl. Sci. 56 (3) (2009) 1459–1464.
[11] R. Armstrong, S.M. McDaid, M.J. Cooper, G. Harding, Substance detection systems, SPIE 2092 (1993) 411–416.
[12] G. Harding, Law enforcement technologies, SPIE 2511 (1995) 64–70.
[13] R.D. Luggar, J.A. Horrocks, R.D. Speller, R.J. Lacey, Low angle X-ray scatter for explosives detection: a geometry optimization, Appl. Radiat. Isot. 48 (1998) 215–224.
[14] P.C. Johns, M.J. Yaffe, Coherent scatter in diagnostic radiology, Med. Phys. 10 (1983) 40–50.
[15] R. Caminiti, V. Rossi Albertini, The kinetics of phase transitions observed by energy-dispersive X-ray diffraction, Int. Rev. Phys. Chem. 18 (1999) 263–299.
[16] B. Kämpfe, R. Arnhold, Application of energy-dispersive X-ray diffraction for mobile analysis, Proc. EDXRS 2002 (2002)8 (June 2002, 16–21, Berlin, Germany).
[17] R. Görgl, P. Wobrauschek, Ch. Streli, H. Aiginger, M. Benedikt, Energy-dispersive measurement and comparison of different spectra from diffraction X-ray tubes, X-ray Spectrom 24 (1995) 157–162.